Direct Observation of *para*-Xylylene as the Decomposition Product of the *meta*-Xylyl Radical Using VUV Synchrotron Radiation

Patrick Hemberger,*[,†] Adam J. Trevitt,*[,‡] Edward Ross,[§] and Gabriel da Silva*[,§]

[†]Molecular Dynamics Group, Paul Scherrer Institute, 5232 Villigen PSI, Switzerland
[‡]School of Chemistry, University of Wollongong, New South Wales 2522, Australia
[§]Department of Chemical and Biomolecular Engineering, The University of Melbourne, Victoria 3010, Australia

S *Supporting Information*

ABSTRACT: Xylyl (methylbenzyl) radicals are important combustion intermediates, formed in the pyrolysis and oxidation of xylenes and other substituted aromatic fuel additives. We have used VUV synchrotron radiation and imaging photoelectron photoion coincidence (iPEPICO) spectroscopy techniques to identify *para*-xylylene as the dominant stable C_8H_8 product arising from thermal decomposition of the *meta*-xylyl radical. A complex rearrangement from a *meta*- to a *para*-substituted aromatic, supported by quantum chemical calculations, can rationalize the observed reaction products. This work provides the first experimental evidence for the pyrolysis products of the *meta*-xylyl radical and can explain why the decomposition of this radical is considerably slower than that of the *ortho* and *para* isomers. This study emphasizes the utility of VUV synchrotron radiation and iPEPICO spectroscopy to tackle the reaction mechanism of combustion-relevant processes.

SECTION: Spectroscopy, Photochemistry, and Excited States
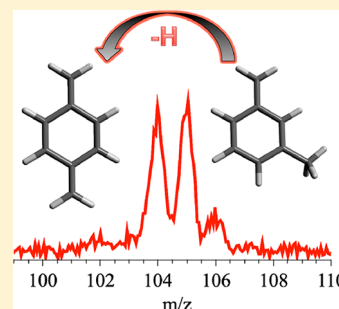
Aromatic hydrocarbons are key components of liquid transportation fuels, typically comprising around a quarter (and as high as 45% in some countries[1]) of gasoline. Aromatics are essentially required in gasoline due to their high octane ratings, and because most countries have regulated benzene out of fuels, these aromatics are in the form of (poly)alkylated benzene derivatives. Toluene is usually the most abundant aromatic found in gasoline and is commonly employed as a surrogate fuel for aromatics. Significant quantities of poly-methylbenzenes (such as the xylenes) and larger alkylbenzenes (such as ethylbenzene) are also encountered in gasoline in considerable levels. Importantly, because the octane rating of toluene is among the lowest of the aromatics,[2] it may prove to be a poor general proxy for the aromatic fraction of gasoline. It is imperative, therefore, to understand the combustion properties of aromatic hydrocarbons more complex than toluene. Intriguingly, when more than one methyl substituent is introduced onto the aromatic ring, combustion properties including octane ratings,[2,3] ignition delays,[4,5] and burning velocities[6] are found to vary dramatically with both the number *and* position of the substituents.

Behind toluene, the three xylene isomers are typically the most abundant aromatics found in gasoline. Furthermore, because the *m*- and *p*- isomers have considerably higher octane ratings than toluene, they may prove to be better fuel surrogates. However, there are marked differences in their combustion behavior, and this points to different decomposition processes for the corresponding xylyl radical species (Scheme 1). As one example, the research octane number (RON) of *o*-xylene is a full 25 points lower than that of the *m*- and *p*- isomers,[2] predominantly attributed to the ability of the

Scheme 1
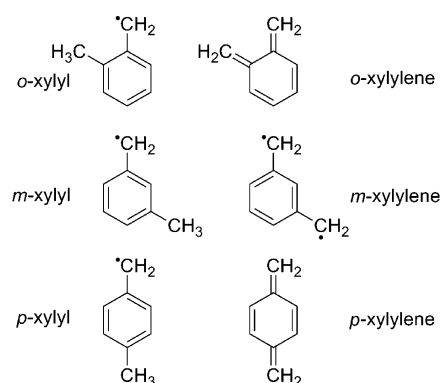
o-xylyl (methylbenzyl) radical to undergo low-temperature chain-branching QOOH radical chemistry.[3] On the other hand, laminar burning velocities of *o*- and *p*-xylene are similar, whereas that of *m*-xylene is considerably slower. This effect has been attributed to the slow decomposition of the *m*-xylyl radical, which is unable to form a conjugated quinodimethide intermediate as in the case of the *o*- and *p*- isomers (see Scheme 1).[5] The *m*-xylyl radical, which is relatively stable toward both oxidation and pyrolysis reactions, can then be thought of as a sink for more reactive free radicals in flames.

The isomeric xylyl ($CH_3C_6H_4CH_2^{\bullet}$) radicals are the key intermediates in xylene combustion. A major limitation to modeling *m*-xylene combustion is that the products of *m*-xylyl radical decomposition are unknown. Fernandez et al.[7] measured rate coefficients for *m*-xylyl radical decomposition in a shock tube using atomic resonance absorption spectroscopy to follow H atom formation. Because the decomposition kinetics were considerably slower than that in the *o*- and *p*- isomers, it was quite reasonably assumed that the diradical *m*-xylylene structure (m-$^{\bullet}CH_2C_6H_4CH_2^{\bullet}$) accounted for the C_8H_8 decomposition product. More recently, da Silva et al.[8] examined the thermochemistry of xylyl radical decomposition, and although *o*- and *p*-xylylenes (o/p-$CH_2{=}C_6H_4{=}CH_2$) were consistent with the products of *o*- and *p*-xylyl radical decomposition, the m-substituted xylylene diradical was far too high in energy to account for the known kinetics of *m*-xylyl radical pyrolysis. Instead, a mechanism akin to the early stages of benzyl radical decomposition[9,10] was proposed, which would allow the *m*-xylyl radical to rearrange to the more fragile *o*- and/or *p*- isomers. In turn, these *o*- and *p*-xylyl isomers subsequently fragment to a conjugated (closed-shell) *o*- or *p*-xylylene with the elimination of a H atom. This process has now been incorporated into detailed kinetic models of aromatic combustion,[11,12] although it remains to be confirmed experimentally, and this experimental shortcoming is addressed here in this Letter.

We have studied *m*-xylyl radical pyrolysis using iPEPICO (imaging photoelectron photoion coincidence) spectroscopy at the VUV (X04DB) beamline of the Swiss Light Source in order to address the uncertainty around its primary decomposition products. We have shown in the past that this technique is excellent for the isomer-selective identification of reactive intermediates and other reaction products.[13−16] In this study, we have used *m*-xylyl bromide (Sigma-Aldrich, Schnelldorf, Germany) to generate the *m*-xylyl radical (C_8H_9, m/z 105) in a pyrolysis source. The radical can then, when sufficiently heated, further fragment into new products, and of particular interest here is the H atom loss product expected at m/z 104 (C_8H_8). The *m*-xylyl radical (m/z 105) and its C_8H_8 product (m/z 104) are unambiguously identified on the basis of mass-selected threshold photoelectron spectra (ms-TPES), with comparison to simulated spectra. This work confirms that the *m*-xylyl radical does not undergo pyrolysis to yield the diradical *m*-xylylene, and instead, we identify *p*-xylylene as the dominant stable C_8H_8 product under our experimental conditions.

Photoionization mass spectra of *m*-xylyl bromide at a range of heating powers are depicted in Figure 1. Even at relatively low heating rates, a signal at m/z 105 appears, attributed to homolysis of the weak C−Br bond in the parent molecule, yielding the *m*-xylyl radical. Applying intermediate pyrolysis power results in the precursor almost fully converting to the *m*-xylyl radical. Only at relatively high pyrolysis temperatures (approximately 1100 K) is m/z 104 detected, assigned as the C_8H_8 product of *m*-xylyl decomposition. We would like to point out that the temperature could not be measured during these experiments; however, in subsequent experiments under similar conditions (distance of the electrodes, resistance, heating power), a pyrolysis temperature of approximately 1100 K is measured by a type C thermocouple. For the other mass spectra at lower heating current, no reliable values can be estimated. It is obvious that the appearance of m/z 104 does not correspond to HBr loss of the precursor because a dependency between the precursor and m/z 104 would have
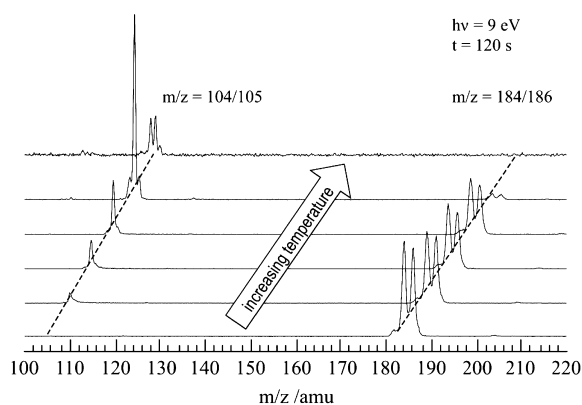

Figure 1. Photoionization mass spectra for *m*-xylyl bromide pyrolysis at increasing temperatures. At lower heating powers, the radical signal at m/z 105 and the precursor (m/z 184/186) are visible. The top trace clearly shows the appearance of the C_8H_8 species (m/z 104).

been observed. Thus, we conclude that the *m*-xylyl radical is the decomposing species. Note that minor peaks can be seen at the highest pyrolysis temperatures corresponding to C_7H_n species at m/z 89−91, which might arise from a slow methyl radical loss channel in the *m*-xylyl radical to yield fulvenallene (*c*-$C_5H_4{=}C{=}CH_2$, m/z 90), followed by H atom addition/loss in the flow (see Scheme 2). Some signal at m/z 106 can also be

Scheme 2
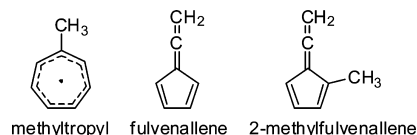
observed at higher temperatures, which could arise from H atom addition to the xylyl radical regenerating *m*-xylene. The appearance of m/z 118 might be due to a recombination of methyl radicals and xylyl radicals and shows that bimolecular reactions only play a subordinate role.

The m/z 105 product of *m*-xylyl bromide pyrolysis can be assigned as the *m*-xylyl radical on the basis of its ms-TPES (Figure 2). A strong progression with a spacing of 60 meV ($\sim$460 cm^{-1}) is clearly visible. The measured adiabatic IE of 7.12 ± 0.01 eV is in excellent agreement with the literature value of 7.12 eV.[17] For the experimental uncertainty, an error of half of the full width at half-maximum (fwhm) of the 0−0 transition was assumed. Rearrangement to one of the other isomers can be unequivocally excluded because *o*- and *p*-xylyl radicals possess adiabatic IEs of 7.07 and 6.96 eV, respectively.[17] This is also in agreement with prior quantum chemical calculations at the G3SX level of theory,[8] which place the adiabatic IE of *m*-xylyl at 7.12 eV, compared to values of 7.10 and 6.96 eV for the respective *o*- and *p*- isomers. As with the parent benzyl radical, it may be possible for *m*-xylyl to rearrange to the methyltropyl radical (structure depicted in Scheme 2).[8,9,18] The IE of the unsubstituted tropyl radical is 6.3 eV, and the value for methyltropyl should be similar but this species does not appear to be present as there are no ion counts below 7 eV in the m/z 105 TPES (Figure 2).[15,19]

A Franck−Condon (FC) simulation convoluted with a Gaussian function (fwhm = 20 meV) matches almost perfectly with the experimental spectrum, showing the activity of two ring-deformation modes mostly associated with C−C−C
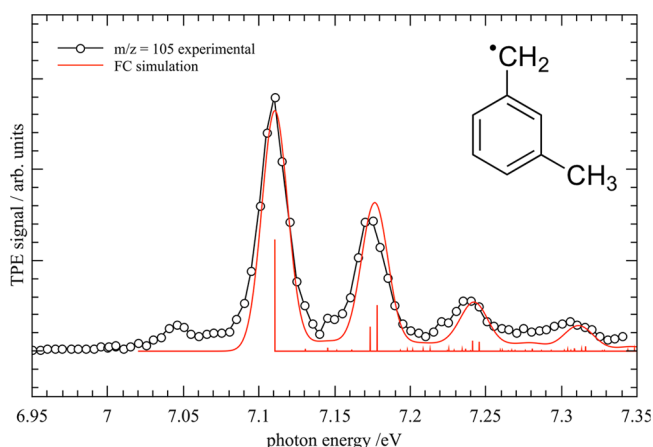
Figure 2. Threshold photoelectron spectrum for the *m/z* 105 species formed in the pyrolysis of *m*-xylyl bromide compared with a Franck–Condon (FC) simulation for the *m*-xylyl radical. The spectrum was recorded under the same conditions as the second highest trace in Figure 1 (*T* is below 1100 K).

bending vibrations. The hot band at around 7.05 eV is not taken into account in the simulation. The geometry change upon ionization and the complete assignment of the band structure will be discussed in more detail in a future publication. Note that neither the *o*- nor the *p*-xylyl radical isomer (adiabatic IEs of 7.07 and 6.96 eV) can be attributed as carrying the band at 7.05 eV.

The identity of the *m/z* 104 channel has also been investigated on the basis of the ms-TPES depicted in Figure 3 and was measured under similar conditions as the top trace in
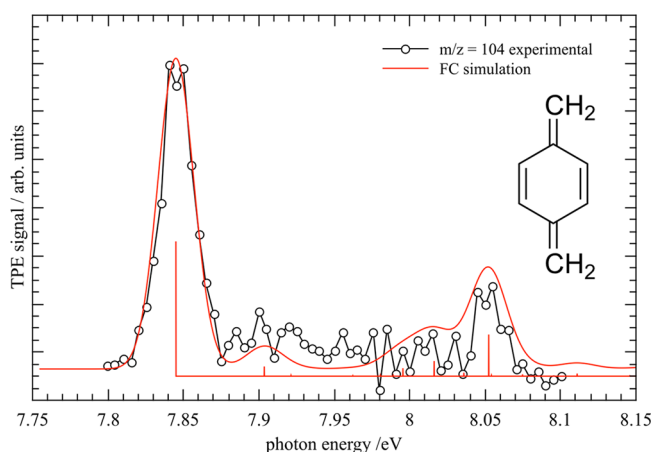

Figure 3. Threshold photoelectron spectrum for the *m/z* 104 product from *m*-xylyl bromide pyrolysis, with comparison to a FC simulation for *p*-xylylene.

Figure 1 (roughly 1100 K) but with an optimized S/N ratio. It is apparent that this pyrolysis product is not the *m*-xylylene diradical, which has a calculated adiabatic IE of 7.29 eV.[8] Comparison with literature adiabatic IEs of the other C_8H_8 isomers *o*-xylylene (7.70 eV),[20] styrene (8.464 eV),[21] *p*-xylylene (7.87 eV),[22] and benzocyclobutene (8.66 eV),[23] confirms undoubtedly that *p*-xylylene is detected and that this is a product of *m*-xylyl decomposition. In order to further substantiate this assignment, the structure of the TPE spectrum was simulated by a FC analysis, showing mostly an activity of C−C−C bending and C−C stretching vibrations. The

simulated spectrum reproduces the experimental spectrum very well, indicating that mass-selected threshold ionization in combination with FC simulations is a versatile tool for the recognition of different isomers of the same composition.

The observation of *p*-xylylene as the thermal decomposition product of the *m*-xylyl radical is consistent with the mechanism put forward by da Silva et al.[8] on the basis of what was a degenerate isomerization process in the parent benzyl radical. We have performed ab initio calculations to extend this mechanism with respect to both the *o*- and *p*- radical isomers at the G4 level of theory, resulting in the energy diagram provided in Figure 4. The *m*-xylyl radical can rearrange to both *o*- and *p*-xylyl via ring contraction to a bicyclic [3.1.0] intermediate, followed by rate-determining ring-opening/ring-closing reactions to produce alternate bicyclic [3.1.0] isomers that can subsequently ring-open to yield the *o*- and *p*-xylyl radicals. The highest barriers for isomerization of *m*-xylyl to the respective *o*- and *p*- isomers are effectively the same, 70 kcal mol⁻¹. From here, the *p*-xylyl radical can readily lose a H atom to provide *p*-xylylene in a barrierless process that is only 63 kcal mol⁻¹ above the originating *m*-xylyl radical. For the *o*-xylyl radical, the analogous reaction also takes place but in this case at 70 kcal mol⁻¹, above *m*-xylyl. Note that although the energetic requirements for isomerization of *m*-xylyl to *o*-xylyl are similar to those for dissociation of *o*-xylyl to *o*-xylylene + H, the overall entropy penalty for the tight isomerization process significantly exceeds that of the loose dissociation reaction, explaining why the *m*-xylyl radical pyrolysis is considerably slower than *o*-xylyl pyrolysis. This does not, however, explain why *p*-xylylene is exclusively detected in our experiments. Note also that theoretical calculations indicate that decomposition to methyl-fulvenallene isomers + H or to fulvenallene + CH_3 requires large barriers (>85 kcal mol⁻¹) and is unlikely to be a significant process, in accord with experiment (see the Supporting Information).

The absence of experimental evidence for any *o*-xylylene as a decomposition product of the *m*-xylyl radical is intriguing. In the final stage of *m*-xylyl radical pyrolysis, the larger barrier for *o*-xylyl versus *p*-xylyl radical dissociation may provide some added impediment to production of the former product, although *o*-xylylene is still likely to form in significant yields. One possibility is that the *o*-xylylene isomer is being formed from *m*-xylyl, but at the required temperatures, it is rapidly undergoing further decomposition. It is known, for instance, that *o*-xylylene can ring-close to benzocyclobutene and isomerize to styrene at temperatures as low as about 1000 K.[24] Styrene was detected in one spectrum (see the Supporting Information) but was not routinely observed. Styrene, the C_8H_8 minimum, lies at 24 kcal mol⁻¹ below *o*-xylylene and is known to decompose with an activation energy of around 80 kcal mol⁻¹.[25,26] Given the overall barrier that would be required to form *o*-xylylene from *m*-xylyl (~70 kcal mol⁻¹), it appears that the reaction product would be able to acquire sufficient energy from the bath gas to also rearrange and fragment on to new products (with an overall barrier estimated at around 55 kcal mol⁻¹). Styrene dissociates to predominantly yield benzene and acetylene,[25–28] neither of which would ionize to any significant extent at the energies used in these experiments (up to 9.0 eV), and further experiments would be required to identify and assign these possible products.

This work has identified *p*-xylylene as the dominant decomposition product of the *m*-xylyl radical on the basis of ms-TPES. This confirms that the *m*-xylyl radical does, indeed,
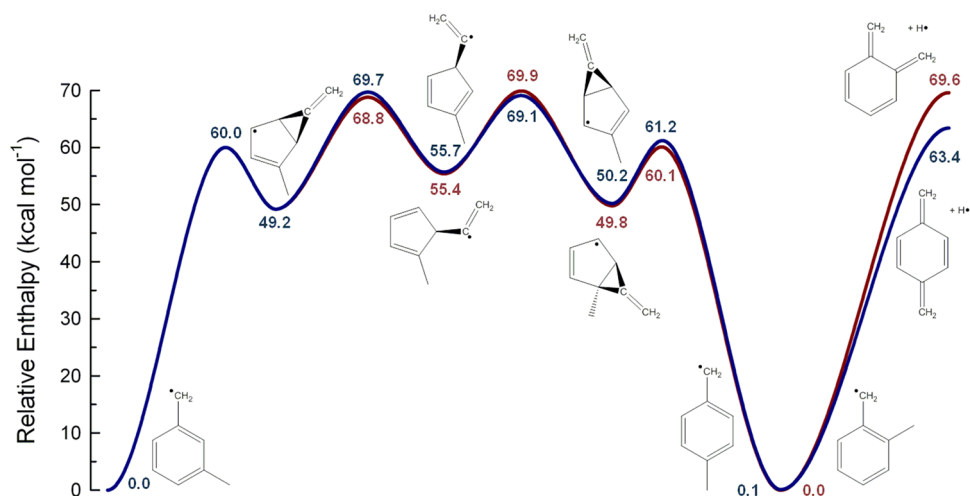
Figure 4. Energy diagram for isomerization and decomposition of the *m*-xylyl radical. Energies are 298 K enthalpies calculated at the G4 level of theory. The blue pathway indicates isomerization to *p*-xylyl, and the red pathway indicates isomerization to *o*-xylyl.

undergo a complex and unique rearrangement process instead of fragmenting to a diradical *m*-xylylene. Our findings support the inclusion of this putative pathway in recent combustion models for aromatic fuels and can explain why different burning velocities[6] are found for the three xylene isomers. More generally, this work highlights the power of VUV synchrotron radiation coupled with iPEPICO spectroscopy in unraveling the products and mechanisms of important yet elusive combustion processes. We plan to use these methods especially when mass analysis is not sufficient enough to distinguish isomers of very similar ionization potentials.

METHODS

Experimental Section. The experimental work was carried out at the iPEPICO endstation of the VUV beamline of the Swiss Light Source. Only a brief summary of the setup is given, and we refer the reader to previous publications.[29−31] Bending magnet radiation is collimated onto a grazing incidence monochromator, working with a 600 mm^{-1} grating, and focused downstream onto a 200 μm exit slit, providing a resolution of 5 meV measured at 11s′ of the argon Rydberg series (15.764 eV). A differentially pumped gas filter (Ar, Kr, Ne) or a MgF$_2$ window is used to suppress the higher-order radiation of the grating. Ions are detected in a time-of-flight mass spectrometer, and electrons are velocity map imaged in coincidence (iPEPICO), permitting us to measure mass-selected threshold photoelectron spectra. Typically, an electron resolution of 5 meV was selected. The *m*-xylyl radical and its decomposition products were generated in a resistively heated SiC tube,[32] where temperatures of around 1300 K can be achieved. Commercially available *m*-xylyl bromide (96%) was vaporized in a temperature-controlled bubbler, operating at 70 °C in an argon carrier gas stream (30−50 mbar backing pressure). After expansion through a 150 μm pinhole, the mixture enters the SiC reactor. No molecular beam skimmer was utilized in these measurements to increase the S/N ratio, making the determination of flows, cooling, residence times, and pressures in the reactor difficult because the conditions are between effusive and supersonic expansion. On the basis of the assumption of 10^{13} particles cm^{-3}, a pressure of roughly 10^{-4} mbar in the reactor can be estimated. Residence times in the reactor might be on the order of a several hundred microsecond

up to a few milliseconds.[33] Infrared (Bruker, Vertex 70v) and NMR (Bruker, Topspin, 300 MHz) spectroscopy was performed on the *m*-xylyl bromide sample to confirm its purity, and no evidence of contamination from the *o*- or *p*-isomers are present (see the Supporting Information).

Theory. Calculations were performed using the G4 composite theoretical method.[34] For G4 theory, optimized structures and zero-point energies were determined at the B3LYP/6-31G-(2df,p) level of theory, followed by a series of higher-level single-point energy calculations. A CCSD(T) energy calculation was performed with the 6-31G(d) basis set, which was subsequently corrected for basis set truncation and core electron correlation by incorporating a sequence of MP2 and MP4 energies as well as a complete basis set Hartree−Fock energy. The final G4 energy also contained an empirical higher-level correction term. G4 theory achieved a mean unsigned deviation of 0.83 kcal mol^{-1} for 454 energies in the G3/05 test set[34] and 1.36 kcal mol^{-1} for a set of 76 barrier heights.[35] All calculations were performed using Gaussian 09.[36] Coordinates for optimized stationary points are provided as Supporting Information. FC simulations were performed using optimized geometries of the neutral and ion and applying the program ezSpectrum.[37]

ASSOCIATED CONTENT

ⓢ Supporting Information
Coordinates for optimized stationary points, energy diagrams for *m*-xylyl dissociation to fulvenallene + CH$_3$ and 2/3-methylfulvenallene + H, and additional spectra are given. This material is available free of charge via the Internet at http://pubs.acs.org.

AUTHOR INFORMATION

Corresponding Author
*patrick.hemberger@psi.ch (P.H.); adamt@uow.edu.au (A.J.T.); gdasilva@unimelb.edu.au (G.d.S.).
Notes
The authors declare no competing financial interest.

ACKNOWLEDGMENTS

■ REFERENCES

(1) *Fuel Standard (Petrol) Determination* 2001 (Commonwealth of Australia). http://www.environment.gov.au/atmosphere/fuelquality/standards/petrol.html (2001).

(2) *Knocking Characteristics of Pure Hydrocarbons*; American Petroleum Institute: Washington, DC, 1958.

(3) da Silva, G.; Bozzelli, J. W. On the Reactivity of Methylbenzenes. *Combust. Flame* **2010**, *157*, 2175−2183.

(4) Shen, H.-P. S.; Oehlschlaeger, M. A. The Autoignition of C_8H_{10} Aromatics at Moderate Temperatures and Elevated Pressures. *Combust. Flame* **2009**, *156*, 1053−1062.

(5) Roubauda, A.; Minettia, R.; Socheta, L. R. Oxidation and Combustion of Low Alkylbenzenes at High Pressure: Comparative Reactivity and Auto-Ignition. *Combust. Flame* **2000**, *121*, 535−541.

(6) Farrell, J.; Johnston, R.; Androulakis, I. Molecular Structure Effects On Laminar Burning Velocities At Elevated Temperature And Pressure. *SAE [Tech. Pap.]* **2004**, 2004-01-2936.

(7) Fernandes, R. X.; Gebert, A.; Hippler, H. The Pyrolysis of 2-, 3-, and 4-Methylbenzyl Radicals Behind Shock Waves. *Proc. Combust. Inst.* **2002**, *29*, 1337−1343.

(8) da Silva, G.; Moore, E. E.; Bozzelli, J. W. Decomposition of Methylbenzyl Radicals in the Pyrolysis and Oxidation of Xylenes. *J. Phys. Chem. A* **2009**, *113*, 10264−10279.

(9) Cavallotti, C.; Derudi, M.; Rota, R. On the Mechanism of Decomposition of the Benzyl Radical. *Proc. Combust. Inst.* **2009**, *32*, 115−121.

(10) da Silva, G.; Cole, J. A.; Bozzelli, J. W. Thermal Decomposition of the Benzyl Radical to Fulvenallene (C_7H_6) + H. *J. Phys. Chem. A* **2009**, *113*, 6111−6120.

(11) Gudiyella, S.; Malewicki, T.; Comandini, A.; Brezinsky, K. High Pressure Study of m-Xylene Oxidation. *Combust. Flame* **2011**, *158*, 687−704.

(12) Diévart, P.; Kim, H. H.; Won, S. H.; Ju, Y.; Dryer, F. L.; Dooley, S.; Wang, W.; Oehlschlaeger, M. A. The Combustion Properties of 1,3,5-Trimethylbenzene and a Kinetic Model. *Fuel* **2012**, *109*, 125−136.

(13) da Silva, G.; Trevitt, A. J.; Steinbauer, M.; Hemberger, P. Pyrolysis of Fulvenallene (C_7H_6) and Fulvenallenyl (C_7H_5): Theoretical Kinetics and Experimental Product Detection. *Chem. Phys. Lett.* **2011**, *517*, 144−148.

(14) Steinbauer, M.; Hemberger, P.; Fischer, I.; Bodi, A. Photoionization of C_7H_6 and C_7H_5: Observation of the Fulvenallenyl Radical. *ChemPhysChem* **2011**, *12*, 1795−1797.

(15) Fischer, K. H.; Hemberger, P.; Bodi, A.; Fischer, I. Photoionisation of the Tropyl Radical. *Beilstein J. Org. Chem.* **2013**, *9*, 681−688.

(16) Hemberger, P.; Steinbauer, M.; Schneider, M.; Fischer, I.; Johnson, M.; Bodi, A.; Gerber, T. Photoionization of Three Isomers of the C_9H_7 Radical. *J. Phys. Chem. A* **2009**, *114*, 4698−4703.

(17) Hayashibara, K.; Kruppa, G. H.; Beauchamp, J. L. Photoelectron Spectroscopy of the o-, m-, and p-Methylbenzyl Radicals. Implications for the Thermochemistry of the Radicals and Ions. *J. Am. Chem. Soc.* **1986**, *108*, 5441−5443.

(18) da Silva, G.; Cole, J. A.; Bozzelli, J. W. Kinetics of the Cyclopentadienyl + Acetylene, Fulvenallene + H, And 1-Ethynylcyclopentadiene + H Reactions. *J. Phys. Chem. A* **2010**, *114*, 2275−83.

(19) Koenig, T.; Chang, J. C. Helium(I) Photoelectron Spectrum of Tropyl Radical. *J. Am. Chem. Soc.* **1978**, *100*, 2240−2242.

(20) Kreile, J.; Münzel, N.; Schulz, R.; Schweig, A. UV Photoelectron Spectrum of o-Xylylene — Detection of a Low-Energy Non-Koopmans (Shake-Up) Ionization. *Chem. Phys. Lett.* **1984**, *108*, 609−612.

(21) Dyke, J. M.; Ozeki, H.; Takahashi, M.; Cockett, M. C. R.; Kimura, K. A Study of Phenylacetylene and Styrene, And Their Argon Complexes PA−Ar and ST−Ar with Laser Threshold Photoelectron Spectroscopy. *J. Chem. Phys.* **1992**, *97*, 8926−8933.

(22) Koenig, T.; Wielesek, R.; Snell, W.; Balle, T. Helium(I) Photoelectron Spectrum of p-Quinodimethane. *J. Am. Chem. Soc.* **1975**, *97*, 3225−3226.

(23) Brogli, F.; Giovannini, E.; Heilbronner, E.; Schurter, R. Die Photoelektronen-Spektren der Benzocycloalkene. *Chem. Ber.* **1973**, *106*, 961−969.

(24) Chapman, O. L.; Tsou, U. P. E.; Johnson, J. W. Thermal Isomerization of Benzocyclobutene. *J. Am. Chem. Soc.* **1987**, *109*, 553−559.

(25) Grela, M. A.; Amorebieta, V. T.; Colussi, A. J. Pyrolysis of Styrene: Kinetics and Mechanism of the Equilibrium Styrene ↔ Benzene + Acetylene. *J. Phys. Chem.* **1992**, *96*, 9861−9865.

(26) Mueller-Markgraf, W.; Troe, J. Thermal Decomposition of Ethylbenzene, Styrene, And Bromophenylethane: UV Absorption Study in Shock Waves. *J. Phys. Chem.* **1988**, *92*, 4914−4922.

(27) Yu, C. F.; Youngs, F.; Bersohn, R.; Turro, N. J. Photo-dissociation at 193 nm of Cyclooctatetraene and Styrene into Benzene and Acetylene. *J. Phys. Chem.* **1985**, *89*, 4409−4412.

(28) Lee, Y.-R.; Chen, C.-C.; Lin, S.-M. Photoelimination of C_2H_2 and H_2 from Styrene at 193 nm. *J. Chem. Phys.* **2003**, *118*, 9073−9076.

(29) Johnson, M.; Bodi, A.; Schulz, L.; Gerber, T. Vacuum Ultraviolet Beamline at the Swiss Light Source for Chemical Dynamics Studies. *Nucl. Instrum. Methods Phys. Res., Sect. A* **2009**, *610*, 597−603.

(30) Bodi, A.; Hemberger, P.; Gerber, T.; Sztaray, B. A New Double Imaging Velocity Focusing Coincidence Experiment: i2PEPICO. *Rev. Sci. Instrum.* **2012**, *83*, 083105/1−083105/8.

(31) Bodi, A.; Johnson, M.; Gerber, T.; Gengeliczki, Z.; Sztaray, B.; Baer, T. Imaging Photoelectron Photoion Coincidence Spectroscopy with Velocity Focusing Electron Optics. *Rev. Sci. Instrum.* **2009**, *80*, 034101/1−034101/7.

(32) Kohn, D. W.; Clauberg, H.; Chen, P. Flash Pyrolysis Nozzle for Generation of Radicals in a Supersonic Jet Expansion. *Rev. Sci. Instrum.* **1992**, *63*, 4003−4005.

(33) Zhang, X.; Friderichsen, A. V.; Nandi, S.; Ellison, G. B.; David, D. E.; McKinnon, J. T.; Lindeman, T. G.; Dayton, D. C.; Nimlos, M. R. Intense, Hyperthermal Source of Organic Radicals for Matrix-Isolation Spectroscopy. *Rev. Sci. Instrum.* **2003**, *74*, 3077−3086.

(34) Curtiss, L. A.; Redfern, P. C.; Raghavachari, K. Gaussian-4 Theory. *J. Chem. Phys.* **2007**, *126*, 084108.

(35) Curtiss, L. A.; Redfern, P. C.; Raghavachari, K. Assessment of Gaussian-4 Theory for Energy Barriers. *Chem. Phys. Lett.* **2010**, *499*, 168−172.

(36) Frisch, M. J.; Trucks, G. W.; Schlegel, H. B.; Scuseria, G. E.; Robb, M. A.; Cheeseman, J. R.; Scalmani, G.; Barone, V.; Mennucci, B.; Petersson, G. A.; et al. *Gaussian 09*, revision B.01; Gaussian Inc.: Wallingford, CT, 2009.

(37) Mozhayskiy, A.; Krylov, A. I. *ezSpectrum*. http://iopenshell.usc.edu/downloads (2008).